

Factorizing Hidden Particle Production Rates

Philipp Klose^{*1}

¹Institut für theoretische Physik, Universität Bern

7th March 2022

Abstract

A method is proposed to streamline the computation of hidden particle production rates by factorizing them into i) a model-independent SM contribution, and ii) a observable-independent hidden sector contribution. The SM contribution can be computed once for each observable and re-used for a wide array of hidden sector models, while the hidden sector contribution can be computed once for each model, and re-used for a wide array of observables. The SM contribution also facilitates extracting model independent constraints on hidden particle production. The method is compatible with effective field theory (EFT) and simplified model approaches. It is illustrated by factorizing the rate of charged kaon decays into a charged lepton and a number of hidden particles, and a single form factor F_ℓ is found to parametrize the impact of general hidden sectors. We derive model-independent constraints for the form factor F_e that governs decays into positrons and hidden particles.

Contents

1	Introduction	2
2	Inclusive production rates	3
2.1	Factorization	5
2.2	Feynman rules	6
3	Illustrative example: Inclusive $K^+ \rightarrow \ell^+$ decays	7
3.1	Reduced matrix elements	8
3.2	Hidden current matrices	11
4	Conclusion and outlook	12
	Appendices	14

*pklose@itp.unibe.ch

1 Introduction

Since the Standard Model (SM) of particle physics is known to be incomplete, the search for physics beyond the Standard Model, and in particular for new particles, is an integral part of modern high energy physics. Focusing on searches at collider and fixed target experiments, the phenomenology of candidate particles crucially depends on whether or not they are light enough to be produced at current generation experiments. Light new particles are more strongly constrained, and they can only couple very feebly to the SM.

In recent years, a significant program of searches for such feebly interacting new particles has begun to emerge [1–4]. Relevant constraints can be obtained from high intensity data sets of CMS [5–7] and ATLAS [8], from flavour physics experiments such as LHCb [9–15] or Belle-II [16–18], and from high luminosity runs of the Large Hadron Collider [19]. There is also a number of ongoing and proposed searches at low-energy fixed target experiments such as NA62 [20–26], KOTO [27–29], SeaQuest [30, 31], or SHiP [1], and further complimentary constraints can be obtained from searches at dedicated long-lived particle experiments [32] such as MATHUSLA [33, 34], FASER [35, 36] and CODEX-b [37].

In spite of these searches, numerous viable hidden sector models still predict a large variety of hidden particle candidates. Examples include axion-like particles (ALPs) [38–45], heavy neutral leptons (HNLs) [1, 3, 46], and new vector Bosons [45, 47, 48]. Since standard perturbative methods of computing predictions for the relevant observables (i.e. hidden particle production, scattering, and decay rates) depend on detailed knowledge of the number and the properties of the hidden fields that are presumed to exist as well as their interactions, this poses a challenge for the model independent interpretation of the experimental constraints.

In recent years, effective field theories (EFTs) such as Standard Model effective field theory [49, 50] and Higgs effective field theory [51–54] have become a standard tool for extracting model independent constraints on the SM coupling to *heavy* new particles [55–59]. Due to this success, some effort has been put towards constructing EFTs that also account for light new particles. For instance, there are a number of EFTs that couple the SM to specific candidate particles such as ALPs [60], HNLs [61, 62], or dark photons [63], as well as generic dark matter candidates [64–67]. EFTs are also commonly used to describe non-relativistic interactions between the SM and dark matter candidates [68–76]. Finally, there has been significant work to create a comprehensive framework for constructing *portal effective theories* (PETs) that systematically extend EFTs of the SM by coupling them to generic hidden particles while making only a minimal number of assumptions [77]. Another approach for extracting model independent bounds consists in constructing so-called “simplified models”, which are designed to capture certain features of realistic SM extensions in a minimalist and therefore more generic setup. Simplified models have become popular *e.g.* within the context of searches for particles that are on the cusp of being collider accessible [78, 79] and dark matter candidates [65, 80]. However, while both EFTs and simplified models are useful for studying generic features of hidden sectors, it is not always straightforward to translate the resulting constraints into hard constraints that are applicable to realistic SM extensions.

In this work, we focus on the computation of hidden particle production rates. We argue that some of the challenges associated with establishing model independent constraints can be ameliorated by factorizing these production rates into a product of i) model-independent

“reduced matrix elements” that depend only on SM interactions and ii) observable-independent “hidden current correlation matrices” that capture the impact of general hidden sectors. As we will show, this factorization is completely generic and relies only on a minimal set of assumptions.

Using the reduced matrix elements, it is possible to derive model-independent “master formulae” for a wide range of observables that parametrize the impact of general hidden sectors via a number of generic form factors. The master formulae can be fitted to experimental data in order to extract model-independent constraints on the form factors. In addition, it is possible to use the hidden current correlation matrices in order to translate the form-factor constraints into more specific constraints on the individual parameters of a given hidden sector model. One major advantage of this two-step procedure is that it divides the workload required for computing hidden particle production rates into two largely independent packages: On the one hand, the hidden current correlation matrices depend only on hidden sector physics and can be computed without having to account for the intricacies of SM model physics or collider phenomenology. On the other hand, the master-formulae depend only on SM physics, and can be computed without having to specify the feature of the hidden sector. This division also makes it possible to mix and match results in a more transparent and systematic way while minimizing the need for re-doing computations in order to adapt a given result to a new model.

In order to make use of the factorization procedure, it is necessary to supply a comprehensive list of relevant portal operators that can mediate a given production process. In principle, any EFT that accounts for the presence of light hidden particles can be used to provide such a list. However, the PET framework is particularly well suited for this task, since it makes only minimal assumptions about the symmetries obeyed by the portal interactions and about the internal structure of the hidden sector, while also accounting for the presence of any additional heavy new particles. When combined with an appropriately constructed list of portal operators, the factorization approach is a powerful tool for establishing model independent constraints on hidden sectors. It effectively extends the EFT approach by providing a description that accounts for both light *and* heavy new particles.

The remainder of this paper is structured as follows: In section 2, we provide a short proof of the factorization rule, and derive the general recipes for computing the reduced matrix elements and correlation matrices. In section 3, we illustrate the procedure by considering the example of charged Kaon decays $K^+ \rightarrow \ell^+ X$ into a charged lepton and a number of hidden sector particles. To do so, we first compute a model-independent master amplitude that encodes the impact of generic hidden sectors using a single form factor F_ℓ , and then show how to compute this form factor for an example model that couples the SM to a number of hidden Fermions. We also extract model-independent upper bounds on the form factor F_e that governs charged kaon decays $K^+ \rightarrow e^+ X$ into a positron and a number of hidden particles. Section 4 concludes the paper.

2 Inclusive production rates

In this section, we demonstrate the factorization of inclusive hidden sector production rates into a product of reduced matrix elements M_d and hidden sector correlation matrices J^{de} . Although

the proof is not complicated, it also serves as a derivation of the diagrammatic expressions for both quantities. In the interest of full generality, we consider a generic theory that is composed of a visible sector A and a hidden sector B ,

$$\mathcal{L} = \mathcal{L}_A + \mathcal{L}_B + \mathcal{L}_{\text{portal}} , \quad \mathcal{L}_{\text{portal}} = \sum_d \epsilon \mathcal{A}_d \mathcal{B}^d . \quad (1)$$

The two sectors are linked by a number of weak portal interactions whose strength is measured by a small parameter ϵ . Each portal operator is the product of a local operator $\mathcal{A}_d = \mathcal{A}_d[\{\phi_a\}](x)$ constructed from a collection of visible fields $\{\phi_a\}$ and a conjugated local operator $\mathcal{B}^d = \mathcal{B}^d[\{\xi_c\}](x)$ constructed from a collection of hidden fields ξ_b .

We are interested in computing inclusive rates for the production of hidden particles in experimental setups where the hidden particles cannot be observed directly. In this case, only the number and the properties of the visible particles in the final state are known, and the resulting transition rates involve a sum over an infinite number of viable final states,

$$|M|^2 = \sum_{k=1}^{\infty} |M_k|^2 , \quad |M_k(\mathcal{K} \rightarrow \mathcal{P})|^2 = \int d_k^3 \mathcal{Q} \delta^4(K - P - Q) |\mathcal{M}(\mathcal{K} \rightarrow \mathcal{P}; \mathcal{Q})|^2 , \quad (2)$$

where the index k denotes the total number of hidden particles in the final state. The matrix elements

$$\delta^4(K - P - Q) \mathcal{M}(\mathcal{K} \rightarrow \mathcal{P}; \mathcal{Q}) = \langle \mathcal{P}; \mathcal{Q} | \text{iT} | \mathcal{K} \rangle , \quad \delta^4(K) = (2\pi)^4 \delta^4(K) \quad (3)$$

encode the likelihood of transitioning from an initial state

$$|\mathcal{K}\rangle = |\mathbf{k}_1^{s_1} \dots \mathbf{k}_n^{s_n}\rangle , \quad (4)$$

that consists of n visible particles s_i with four-momenta $k_i = (\kappa_i, \mathbf{k}_i)$ into a given final state

$$\langle \mathcal{P}; \mathcal{Q} | = \langle \mathcal{P} | \otimes \langle \mathcal{Q} | , \quad \langle \mathcal{P} | = \langle \mathbf{p}_1^{t_1} \dots \mathbf{p}_m^{t_m} | , \quad \langle \mathcal{Q} | = \langle \mathbf{q}_1^{r_1} \dots \mathbf{q}_k^{r_k} | . \quad (5)$$

that consists of m visible particles t_j with four-momenta $p_j = (\pi_j, \mathbf{p}_j)$ and k hidden particles r_l with four-momenta $q_l = (\omega_l, \mathbf{q}_l)$. Here and in the following, we use the multi-indices $s = (s_1, \dots, s_n)$, $t = (t_1, \dots, t_m)$, and $r = (r_1, \dots, r_k)$ to collectively denote the species and the helicity of each particle. The integration measure

$$d_k^3 \mathcal{Q} = \prod_{l=1}^k \frac{d^3 \mathbf{q}_l}{(2\pi)^3} \frac{1}{2\omega_l} \sum_{r_l} , \quad (6)$$

includes a sum over both the species and the helicity of each hidden particle as well as an integral over its associated phase space. Finally, the sums

$$K = \sum_i k_i , \quad P = \sum_j p_j , \quad Q = \sum_l q_l = K - P \quad (7)$$

denote the total momentum of the visible particles in the initial and final states as well as the corresponding missing momentum.

Most of the relevant production modes for hidden particles involve either decays or scatterings of visible particles. The general sum (2) determines the overall rates for hidden particle production in both of these cases, yielding

$$d\Gamma = \frac{1}{2\kappa_1} |M(k_1 \rightarrow \mathcal{P})|^2 \prod_{j=1}^m \frac{d^3 \mathbf{p}_j}{(2\pi)^3} \frac{1}{2\pi_j}, \quad d\sigma = \frac{1}{4\kappa_1 \kappa_2 v_{12}} |M(k_1, k_2 \rightarrow \mathcal{P})|^2 \prod_{j=1}^m \frac{d^3 \mathbf{p}_j}{(2\pi)^3} \frac{1}{2\pi_j}, \quad (8)$$

where $v_{12} = |v_1 - v_2|$ is the relative velocity of the two initial state particles in the scattering process. Our aim is to show that the inclusive rate $M(\mathcal{K} \rightarrow \mathcal{P})$ factorizes according to

$$|M(\mathcal{K} \rightarrow \mathcal{P})|^2 = \epsilon^2 M_d M_e^\dagger J^{de} + \mathcal{O}(\epsilon^3), \quad (9)$$

where the reduced matrix elements M_d encode the dynamics of the visible sector while the hidden current correlation matrix J^{de} encodes the impact of hidden sectors. We note that, although equation (9) is completely general, its usefulness crucially depends on the size of the small parameter ϵ . However, this is of no concern within the context of hidden sector searches, since higher order corrections are almost always negligible due to the required smallness of the portal coupling. In this case, the factorization equation (9) becomes a very good approximation.

2.1 Factorization

The factorization of the inclusive rate (9) is a corollary of an equivalent factorization of the time-ordered, connected correlation functions

$$\hat{G}_{abc}(\mathcal{X}, \mathcal{Y}, \mathcal{Z}) = \langle 0 | \text{T} \{ \hat{\Phi}_a(\mathcal{X}) \hat{\Phi}_b^\dagger(\mathcal{Y}) \hat{\Xi}_c^\dagger(\mathcal{Z}) \} | 0 \rangle_{\text{conn.}} \quad (10)$$

that capture the dynamics of hidden particle production. Here and in the following, the average $\langle 0 | \circ | 0 \rangle_{\text{conn.}}$ is defined to include only connected diagrams. In order to avoid superfluous notational clutter, we have defined the multi-field operators

$$\hat{\Phi}_a(\mathcal{X}) = \prod_{i=1}^n \phi_{a_i}(x_i), \quad \hat{\Xi}_a(\mathcal{X}) = \prod_{l=1}^k \xi_{a_l}(x_l), \quad a = (a_1, \dots, a_n), \quad \mathcal{X} = (x_1, \dots, x_n). \quad (11)$$

We also define the corresponding momentum-space operators

$$\Phi_a(\mathcal{K}) = \int d_n^4 \mathcal{X} e^{i\mathcal{X}\mathcal{K}} \hat{\Phi}_a(\mathcal{X}), \quad d_n^4 \mathcal{X} = \prod_{i=1}^n d^4 x_i, \quad \mathcal{X}\mathcal{K} = \sum_{i=1}^n x_i k_i. \quad (12)$$

Expanding the path-integral of the full theory to leading order in ϵ , one immediately finds that the above correlation functions factorize according to

$$\hat{G}_{abc} = -i\epsilon \int d^4 x \hat{G}_{ab;d} \hat{F}_{c;d} + \mathcal{O}(\epsilon^2), \quad \hat{G}_{ab;d} = i \langle 0 | \text{T} \{ \hat{\Phi}_a(\mathcal{X}) \hat{\Phi}_b^\dagger(\mathcal{Y}) \mathcal{A}_d(x) \} | 0 \rangle_{\text{conn.}}^{\epsilon \rightarrow 0}, \quad (13)$$

where the reduced correlation function $\hat{G}_{ab;d}$ only depends on physics of the visible sector, while the form factor

$$\hat{F}_{c;d} = i \langle 0 | \text{T} \{ \hat{\Xi}_c^\dagger(\mathcal{Z}) \mathcal{B}^d(x) \} | 0 \rangle_{\text{conn.}}^{\epsilon \rightarrow 0}. \quad (14)$$

encodes the impact of hidden sectors. Moving on to momentum space, this gives

$$G_{abc} = \langle 0 | \text{T} \{ \Phi_a(\mathcal{K}) \Phi_b^\dagger(\mathcal{P}) \Xi_c^\dagger(\mathcal{Q}) \} | 0 \rangle_{\text{conn.}} = -i \epsilon G_{ab;d}(\mathcal{K}, \mathcal{P}) \mathcal{F}_{c;d}(\mathcal{Q}) + \mathcal{O}(\epsilon^2), \quad (15)$$

where the momentum space versions of the reduced Greens functions and the hidden sector form factors are

$$\delta^4(K - P - Q) G_{ab;d} = \int d^4x d_n^4 \mathcal{X} d_m^4 \mathcal{Y} e^{i(\mathcal{K}\mathcal{X} - \mathcal{P}\mathcal{Y} - qx)} \hat{G}_{ab;d}, \quad (16a)$$

$$\delta^4(q - Q) F_{c;d} = \int d^4x d_k^4 \mathcal{Z} e^{i(qx - Q\mathcal{Z})} \hat{F}_{c;d}. \quad (16b)$$

In order to translate the factorization equation (15) into a statement about the inclusive transition rate (2), we apply the Lehmann-Symanzik-Zimmermann (LSZ) reduction formula to (3). Using the multi-field notation, this gives

$$i \mathcal{M}(\mathcal{K} \rightarrow \mathcal{P}; \mathcal{Q}) = \mathcal{E}^a \bar{\mathcal{E}}^b \bar{\mathcal{E}}^c G_{abc}, \quad \mathcal{E}^a = \prod_i Z_{a_i}^{-1/2} \epsilon^{b_i} G_{b_i a_i}^{-1}, \quad \bar{\mathcal{E}}^a = \prod_i Z_{a_i}^{-1/2} \bar{\epsilon}^{b_i} G_{b_i a_i}^{-1}, \quad (17)$$

where the amputating factors $\mathcal{E}^a = \mathcal{E}^a(s, \mathcal{K})$ and $\bar{\mathcal{E}}^a = \bar{\mathcal{E}}^a(s, \mathcal{K})$ consist of the standard wavefunction renormalization factors Z_{a_i} , the initial and final state polarization vectors $\epsilon^{a_i} = \epsilon^{a_i}(s_i, k_i)$ and $\bar{\epsilon}^{a_i} = \bar{\epsilon}^{a_i}(s_i, k_i)$, and the inverse propagators $G_{b_i a_i}^{-1}(k_i)$.¹ With these definitions in place, inserting equations (15) and (17) into equation (2) finally yields equation (9), where

$$i M_d = \mathcal{E}^a \bar{\mathcal{E}}^b G_{ab;d}, \quad J_{de} = \sum_{k=1}^{\infty} \int \mathcal{D}_k \mathcal{Q} \delta^4(q - Q) J_d J_e^\dagger, \quad i J_d = i J_d(\mathcal{Q}, r) = \bar{\mathcal{E}}^c F_{c;d}. \quad (18)$$

The external current correlation matrix J_{de} fully encodes the impact of hidden sectors. Since the integration $\sum_k \int \mathcal{D}_k \mathcal{Q}$ in the definition of J_{de} includes a sum over the species and the helicities of the hidden particles in the final state, the correlation matrix

$$J_{de} = \sum_{k=1}^{\infty} \sum_r J_{de}^r \quad (19)$$

can be written as an infinite sum of terms $J_{de}^r = J_{de}^r(Q)$ that capture the contribution associated with each individual final state. Notice also that M_d and J_d (and with them J_{de}) can, depending on the precise structure of the corresponding portal operator, carry free Lorentz and spinor indices. For example, if the theory contains a portal operator $\mathcal{A}_\mu \mathcal{B}^\mu = \psi \sigma_\mu \psi^\dagger v^\mu$ that couples a pair of visible Fermions $\mathcal{A}_\mu = \psi \sigma_\mu \psi^\dagger$ to a hidden vector particle $\mathcal{B}^\mu = v^\mu$, then the corresponding reduced matrix element M^μ and hidden currents J_μ carry free Lorentz indices that are to be contracted with each other.

2.2 Feynman rules

The expressions (16) and (18) define series of Feynman diagrams that can be used to compute the reduced matrix elements M_d as well as the hidden currents $J_d(r, \mathcal{Q})$ associated with each viable hidden sector final state.

¹ Recall that the multi-indices $s = (s_1, \dots, s_n)$ collectively denote the species and the helicity of each *particle*, while the multi-indices $a = (a_1, \dots, a_n)$ collectively denote the type of each *field*. Each a_i runs over all available fields present in the theory, and the polarization vectors are defined such that $\epsilon^{a_i}(s_i, k_i) = 0$ in cases where s_i denotes a particle that is not produced by the field associated with the index a_i .

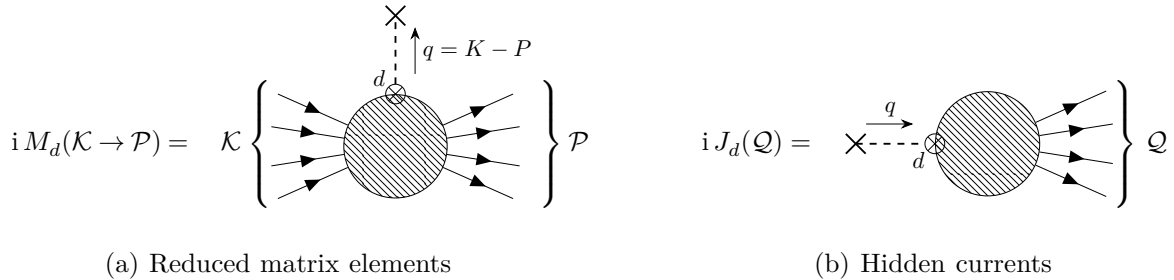


Figure 1: Diagrams for computing the reduced matrix elements M_d and the hidden currents J_d . Both are given as the sum of all available connected and amputated Feynman diagrams with the appropriate number and kind of particles in the initial and final states. The crossed dot denotes the required portal vertex, and the dashed line denotes the relevant missing momentum in- and outflow. Aside from this portal vertex, diagrams for M_d diagrams only contain vertices and propagators associated with visible fields and interactions, while diagrams for J_d only contain vertices and propagators associated with hidden fields and interactions.

Figure 1 shows the diagrammatic expansions for both M_d and J^d . As in the case standard S-matrix element computations, they are given as a sum of all available connected and amputated Feynman diagrams with the appropriate number and kind of particles in the initial and final states, where M_d diagrams only contain vertices and propagators associated with visible fields and interactions while J_d diagrams only contain vertices and propagators associated with hidden fields and interactions. The main difference compared to the recipe for standard S-matrix elements is that all relevant diagrams have to contain exactly one portal vertex that is constructed from either the “visible” part \mathcal{A}_d (in the case of M_d) or the “hidden” part \mathcal{B}^d (in the case of J_d) of the corresponding portal operator.

The rules for constructing these portal vertices are largely the same as those for constructing standard vertices. (i.e. symmetrize the operator under exchange of identical fields, go to momentum space, strip away all fields, and multiply by an overall factor of i .) However, there are two differences: First, and in complete analogy to the composite operators \mathcal{A}_d and \mathcal{B}^d , the portal vertices may carry free Lorentz and spinor indices, which result in M_d and J^d likewise carrying such free indices. Second, both portal vertices do not conserve four-momentum in the strict sense. Rather, the appropriate sum of all ingoing and outgoing momenta has to be equal to some missing momentum q . This is depicted symbolically using a dashed line (*cf.* figure 2). The missing momentum is outflowing for M_d , so that $q = K - P$, and it is inflowing for J_d , so that $q = Q$.

3 Illustrative example: Inclusive $K^+ \rightarrow \ell^+$ decays

To illustrate the factorization procedure as well as the computation of the reduced matrix elements and hidden currents, we consider the production of hidden particles in inclusive $K^+ \rightarrow \ell^+ X$ decays, where X denotes any collection of hidden particles. There already exists a model-independent master-formula for the production rate of generic spin $1/2$ particles in this type of charged kaon decay [77], and the present computation improves this result by

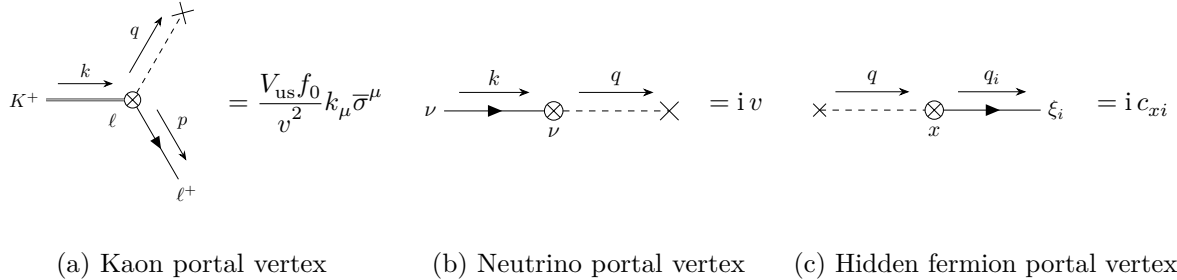


Figure 2: Feynman rules for portal vertices that appear in the example computation of inclusive $K^+ \rightarrow \ell^+$ decay rates. The first vertex figure 2a determines the size of the reduced matrix element M^ℓ , while the second vertex figure 2b determines the size of M^ν . Both contribute at the same order because M^ν is also suppressed by the smallness of the required additional Fermi-theory vertex associated with $K^+ \rightarrow \ell^+ \nu$ decays. The third vertex figure 2c determines the size of the hidden currents J^ℓ and J^ν , and is used in section 3.2.

accounting for the production of hidden particles with different spins as well as the production of multiple hidden particles via the same decay process.

3.1 Reduced matrix elements

The primary input required to factorize inclusive matrix elements according to (9) is an exhaustive list of all relevant portal operators. Here, we use the list compiled in [77], which encompasses all leading operators that couple the SM to a single hidden particle of spin 0, $1/2$, or 1 at the strong scale. The sector of the portal Lagrangian that is relevant for $K^+ \rightarrow \ell^+ X$ decays is

$$\mathcal{L}_{\text{portal}} \supset -v\nu\Xi_\nu + \frac{V_{\text{us}}}{v^2} Q_\mu \Xi_\ell^\dagger \bar{\sigma}^\mu \ell, \quad Q_\mu = s^\dagger \bar{\sigma}_\mu u, \quad (20)$$

where u and s are the up- and strange quark fields, $\ell = e, \mu$ is a charged lepton field, and ν is the corresponding SM neutrino field. Following two-component notation of [81], the SM Fermion fields are taken to be left-handed Weyl spinors. $v = 174.10358 \pm 0.00004 \text{ GeV}$ is the vacuum expectation value of the Higgs Boson and $|V_{\text{us}}| = 0.2252 \pm 0.0008$ is the u-s element of the Cabibbo-Kobayashi-Maskawa matrix [82]. The small parameter ϵ has been re-absorbed into the operators Ξ_ν, Ξ_ℓ , which now take on the role of the generic local operators $\epsilon \mathcal{B}^d$. It is not necessary to specify their detailed shape in order to compute the reduced matrix elements. However, we note that, although the master formula that results from using the portal Lagrangian (20) is largely model-independent, the factorization procedure outlined here can also be used to obtain an even more general master formula by including additional sub-leading portal operators. A collection of the relevant interactions is given e.g. in [61, 62].

Given the portal Lagrangian (20), the resulting coupling of hidden sectors to the pseudo-scalar mesons is captured by the portal chiral perturbation theory (χ PT) action constructed in [77]. We work at leading order in the χ PT power counting, at tree-level, and neglect electromagnetic corrections. At this level of accuracy, the coupling of the operator Ξ_ℓ to charged

kaons can be obtained by replacing the quark bilinears according to [77, 82, 83]

$$Q_\mu \rightarrow f_0 \partial_\mu K^+ , \quad f_0 = 77.85 \pm 0.15 \text{ MeV} , \quad (21)$$

where f_0 is the kaon decay constant. This replacement yields the “visible” portal vertex depicted in figure 2a, while neutrino portal operator in (20) yields the additional vertex depicted in figure 2b.

In general, there is one reduced matrix element for each portal operator. Since there are two relevant portal operators, there are also two reduced matrix elements M_ℓ and M_ν . Using the Feynman rules for two-component spinors given in [81, 84], one finds the leading order expressions²

$$M_\nu^\alpha = i \frac{f_0 V_{\text{us}}}{v q^2} (\sigma_\nu \bar{\sigma}_\mu)^{\alpha\beta} y_\beta^\ell(p, t) q^\nu k^\mu , \quad M_\ell^{\dot{\alpha}} = -i \frac{f_0 V_{\text{us}}}{v^2} (\bar{\sigma}_\mu)^{\dot{\alpha}\beta} y_\beta^\ell(p, t) k^\mu , \quad (22)$$

where y^ℓ is the two-component polarization vector of the final state lepton, $k = (\kappa, \mathbf{k})$ is the kaon four-momentum, $p = (\pi, \mathbf{p})$ is the lepton four-momentum, and $q = k - p$ is the missing momentum. The free spinor indices α and $\dot{\alpha}$ are to be contracted with the external current correlation matrices. Summing over the available ℓ^+ spin polarizations, the resulting inclusive rate for $K^+ \rightarrow \ell^+$ decays is

$$\sum_t |M(k \rightarrow p)|^2 = \sum_t \left(M_\ell^{\dot{\alpha}} M_\ell^{\dagger\beta} J_{\beta\dot{\alpha}}^{\ell\ell} + M_\nu^\alpha M_\nu^{\dagger\dot{\beta}} J_{\dot{\beta}\alpha}^{\nu\nu} + 2 \text{Re} M_\nu^\alpha M_\ell^{\dagger\beta} J_{\beta\alpha}^{\ell\nu} \right) \quad (23a)$$

$$= \left| \frac{f_0 V_{\text{us}}}{v^2} \right|^2 \frac{2(pk)(qk) - (pq)k^2}{k^2} F_\ell(x_q) . \quad (23b)$$

The impact of hidden sector contributions is encoded by the form factor

$$x_q F_\ell(x_q) = \text{tr}_D \left\{ q^\nu \bar{\sigma}_\nu J^{\ell\ell} - 2 \frac{v}{q} \text{Re} q J^{\ell\nu} + \frac{v^2}{q^2} q^\rho \sigma_\rho J^{\nu\nu} \right\} , \quad x_q = \frac{q^2}{m_K^2} , \quad (24)$$

where tr_D is the trace taken with respect to the (un)dotted spinor indices. Since the Levi-Civita tensor is used to raise and lower indices associated with the same chirality, $V^\alpha = \epsilon^{\alpha\beta} V_\beta$, one has $\text{tr}_D \{ J^{\ell\alpha} \} = \epsilon^{\alpha\beta} J_{\beta\alpha}^{\ell\alpha}$. This gives the partial decay width

$$\frac{d\Gamma_\ell}{dx_q} = 4\pi m_K |V_{\text{us}}|^2 \left(\epsilon_{\text{EW}} \frac{m_K}{4\pi f_0} \right)^2 \rho \frac{F_\ell(x_q)}{2\pi} , \quad \epsilon_{\text{EW}} = \frac{f_0^2}{v^2} , \quad (25)$$

where

$$\rho(x_\ell, x_q) = \frac{1}{2} (x_\ell + x_q - (x_\ell - x_q)^2) \sqrt{\left(\frac{1 - x_\ell - x_q}{2} \right)^2 - x_\ell x_q} , \quad x_\ell = \frac{m_\ell^2}{m_K^2} \quad (26)$$

² The leading contribution to M_ℓ is generated by the tree-level diagram that contains only the portal vertex in figure 2a, and the leading contribution to M_ν is generated by the tree-level diagram that contains the SM three-point vertex that mediates $K^+ \rightarrow \ell^+ \nu_\ell$ decays as well as the portal vertex in figure 2b

is a phase-space factor, $m_K = 493.636 \pm 0.007 \text{ MeV}$ is the charged kaon mass, and m_ℓ is the mass of the relevant charged lepton [82]. Comparing equation (25) with the known partial width for $K^+ \rightarrow \ell^+ \nu$ decays [85], one finally obtains the ratio of branching ratios

$$R_\ell(x_q) = \frac{d\mathcal{B}_\ell/dx^2}{\mathcal{B}(K^+ \rightarrow \ell^+ \nu)} = \frac{d\Gamma_\ell/dx^2}{\Gamma(K^+ \rightarrow \ell^+ \nu)} = \frac{\rho(x_\ell, x_q) F_\ell(x_q)}{\rho(x_\ell, 0) 2\pi} . \quad (27)$$

Since the master formula (25) only depends on the overall shape of the portal Lagrangian (20), but not on the specifics of the portal interactions or on the internal structure of the hidden sector, formula (27) is almost completely model independent. In particular, it captures the production of an arbitrary number of hidden particles with arbitrary masses, spins, and interactions. Since we have also allowed for the possibility of higher dimensional SM and portal operators, formula (27) even accounts for the presence of heavy new particles.

Formula (27) can be used to extract model-independent constraints on the size of the form factors $F_\ell(x_q)$. To illustrate how this can be done in practice, we re-interpret the analysis in [25], which uses a missing mass search to establish upper bounds for the branching ratio of charged kaon decays into a positron and a HNL from NA62 data. The HNLs were assumed to decay outside the detector, and the search was hence directed at finding events with a single visible positron in the final state and some finite missing mass $q^2 = m_{\text{miss}}^2 = (k - p)^2$. This setup is a special case of the generic setup that we have considered in this work, where the number and the type of visible particles in the final state is known, while any produced hidden particles are not observed directly.

The analysis in [25] sampled a large number of missing masses in the range $122 \text{ MeV} < m_{\text{miss}} < 465 \text{ MeV}$, searching for candidate events in a bin of width $2\Delta m = 0.3 \text{ MeV}$ centered around the sampled missing mass. For each bin, they extracted an upper bound on the corresponding branching ratio. This upper bound is roughly constant over the entire mass range, and comes out to $\mathcal{B}(K^+ \rightarrow e^+ N) \lesssim 4 \cdot 10^{-9}$. In the following, we interpret this number as a bound on the fractional branching ratio $\Delta\mathcal{B}_e = \Delta x_q \cdot d\mathcal{B}_e/dx_q$, which captures the likelihood of producing a positron and a collection of generic hidden particles with an aggregate missing mass in the range $[x_q - \Delta x_q, x_q + \Delta x_q]$, where $\Delta x_q = (\Delta m/m_K)^2$. Using the known values of $\mathcal{B}(K^+ \rightarrow e^+ \nu_e) = (1.582 \pm 0.007) \cdot 10^{-5}$ and $x_e = m_e^2/m_K^2 \approx 1.07 \cdot 10^{-6}$ [82], this gives the constraint

$$\rho(x_e, x_q) \frac{\langle F_e \rangle 2\Delta x_q}{2\pi} \lesssim 7 \cdot 10^{-11} , \quad 2\Delta x_q \approx 4 \cdot 10^{-7} , \quad 0.06 < x_q < 0.89 , \quad (28)$$

where $\langle F_e \rangle$ is the average of $F_e(x_q)$ taken over the range $[x_q - \Delta x_q, x_q + \Delta x_q]$. To understand how to interpret this constraint, recall that the form factor captures the production of an arbitrary number of hidden particles. Generically, a contribution associated the production of a single hidden particle will include the delta distribution $\delta(q^2 - m_i^2)$, where m_i is the mass of the relevant hidden particle, to ensure that only on-shell particles are produced. In contrast, the phase-space integral $\int d_k Q$ in equation (18) is sufficient to smooth out the contributions associated with the production of two or more hidden particles. Hence, the form factor is of the general shape

$$\frac{F_e(x_q)}{2\pi} = \sum_i A_i \delta(x_q^2 - x_i^2) + B(x_q) , \quad x_i = \frac{m_i^2}{m_K^2} , \quad (29)$$

where the A_i are amplitudes for single particle production and $B(X_q)$ is a smooth function that captures the production of multiple hidden particles. Averaging (29), one finds

$$\frac{\langle F_e \rangle 2\Delta x_q}{2\pi} = \sum_i A_i \Theta(\Delta x_q - |x_i - x_q|) + B(x_q) 2\Delta x_q, \quad (30)$$

where we have used that $\langle B \rangle \approx B$ for sufficiently small bins. Combining this decomposition with the general expression (28), one now obtains separate constraints on the single-particle amplitudes A_i and the multi-particle amplitude $B(x_q)$. The single-particle amplitudes have to obey the model-independent constraint

$$\rho(x_e, x_i) A_i \lesssim 7 \cdot 10^{-11}, \quad 0.06 < x_i < 0.89, \quad (31)$$

while the constraint on the multi-particle amplitude is much less stringent,

$$\rho(x_e, x_q) B(q^2) \lesssim 2 \cdot 10^{-4}, \quad 0.06 < x_q < 0.89. \quad (32)$$

This is to be expected, since a signal for the production of a single hidden particle would appear as a sharp peak that is concentrated into a single bin, while a signal for the production of multiple particles would be spread over a whole range of viable missing masses. While the peak is relatively easy to observe, and therefore constrain, it is more difficult to constrain the spread-out signal.

3.2 Hidden current matrices

In order to translate constraints on the form factors $F_\ell(x_q)$ into more specific constraints, it is necessary to plug in appropriate expressions for the hidden current correlation matrices J^{de} . In this section we demonstrate how to compute general correlation matrices by considering an example case in which the SM couples to a number of left-handed Weyl Fermions ξ_i . Since both Dirac and Majorana Fermions can always be written as a combination of Weyl Fermions, this setup remains quite general. The leading contributions to the portal operators are

$$\Xi_d = \sum_i c_{di} \xi_i, \quad d = \nu, \ell, \quad (33)$$

where the constants $c_{\nu, \ell}$ are model-dependent coupling constants. The corresponding ‘‘hidden’’ portal vertices are depicted in figure 2c.

In general, there is one collection of hidden currents $J^d = J^d(Q, r)$ for each viable hidden sector final state $r = (r_1, \dots, r_k)$, and each of these collections contains one current for each available portal operator. In the concrete case of $K^+ \rightarrow \ell^+ X$ decays this means that there are two hidden currents $J^\nu(Q, r)$ and $J^\ell(Q, r)$ for each final state. Assuming that the hidden sector interactions are perturbatively small, the leading contributions are generated by diagrams without any hidden sector vertices. Since the portal operators in equation (33) contain only a single field operator, the only final states that are viable at this order of accuracy (i.e. neglecting hidden sector interactions) are those with a single hidden Fermion, and no additional hidden particles. The two hidden currents that are associated with this type of final state are given as

$$J_\alpha^\nu(q_1, r_1) = c_{\nu i} y_\alpha^i(\mathbf{q}_1, r_1), \quad J_\alpha^\ell(q_1, r_1) = c_{\ell i} x_\alpha^{i\dagger}(\mathbf{q}_1, r_1), \quad (34)$$

where index $i = i(r_1)$ denotes ξ_i that creates the single-particle final state associated with r_1 . Evaluating the spin sums and the phase-space integration, one obtains the correlation matrices

$$J_{\beta\alpha}^{\nu\nu} = \sum_i \frac{c_{\nu i}^\dagger c_{\nu i}}{2\omega_i} (q_i^\mu \bar{\sigma}_\mu)_{\beta\alpha} 2\pi\delta(q_0 - \omega_i), \quad J_{\beta\alpha}^{\ell\nu} = \sum_i \frac{c_{\ell i}^\dagger c_{\nu i}}{2\omega_i} m_i \epsilon_{\beta\alpha} 2\pi\delta(q_0 - \omega_i), \quad (35a)$$

$$J_{\beta\alpha}^{\ell\ell} = \sum_i \frac{c_{\ell i}^\dagger c_{\ell i}}{2\omega_i} (q_i^\mu \sigma_\mu)_{\beta\alpha} 2\pi\delta(q_0 - \omega_i), \quad (35b)$$

where m_i is the mass of the hidden Fermion ξ_i . Inserting these matrices into the form factor equation (24), one finds

$$\frac{F_\ell(x_q)}{2\pi} = \sum_i U_i^2 \Theta(q_0) \delta(x_q^2 - x_i^2), \quad x_i = \frac{m_i^2}{m_K^2}, \quad U_i^2 = \left| c_{\ell i} - \frac{v c_{\nu i}}{m_i} \right|^2. \quad (36)$$

When combined with the master formula (23b), this result is consistent with the model-independent formula given in [section 6 of 77].

This computation exemplifies a second use of the factorization procedure: In addition to facilitating model-independent constraints on the coupling to hidden sectors, it can also help streamline the derivation of more specific model-dependent constraints. Once the master-formula associated with a given observable has been computed, it does not need to be adjusted anymore, and in order to adapt the result for a new model, it is sufficient to recompute the form-factors $F_\ell(x_q)$. As a final remark, we note that while the form factors $F_\ell(x_q)$ depends on the observable in question, the hidden current correlation matrices in equation (35) do not. They can be provided once and for all, and re-used to compute a wide array of form factors associated with different observables, further reducing the need for re-computing ingredients in order to adapt a known result for a new model or observable.

4 Conclusion and outlook

In this work, we have shown that inclusive hidden particle production rates approximately factorize according to relation (9), and derived recipes for computing the reduced matrix elements M_d and the hidden currents J^d as series of Feynman diagrams. We illustrated the factorization procedure by considering decays $K^+ \rightarrow \ell^+ X$ of charged kaons into charged leptons and a number of hidden particles. The resulting model-independent master formula (25) improves the model-independent formula given in [77] and parametrizes the impact of hidden sectors in terms of a single form factor $F_\ell(x_q)$ that can be constrained in a largely model-independent fashion. To illustrate how to constrain the form factor in practice, we have re-interpreted the analysis of [25] and derived the model-independent bounds (31) and (32).

If the factorization approach is combined with an appropriately general list of portal operators, which can be constructed in a systematic and consistent fashion using *e.g.* the PET framework [77], it correctly accounts for both light *and* heavy new particles. In this case, the factorization approach is strictly more general than the EFT approach, and we have argued that it provides a powerful tool for the model-independent interpretation of hidden sector

searches.

Using the present work as a foundation, there are many potentially interesting avenues for future investigation.

Since the factorization approach relies on lists of portal operators being provided as a necessary input, it will profit greatly from further efforts of extending the EFT approach to also account for light new particles. In particular, the PET framework is well suited for providing the needed lists of portal operators, and constructing further PETs will allow the factorization approach to be applied to a significantly larger variety of observables. At this time, there are PETs that extend the full SM, light effective field theory, which describes the physics of the light SM fields [86–89], and χ PT, which describes the physics of the light pseudoscalar mesons [90–96], by coupling them to a single light new particle of spin 0, $1/2$, or 1 [77]. These PETs also account for the possibility of SM fields coupling to multiple hidden fields with the *same* spin, but they are not sufficient for describing a situation in which the SM couples to multiple hidden particles with *different* spins. Hence, it would be useful to construct a corresponding set of PETs that include the relevant additional portal operators.

Likewise, it would be interesting to construct PETs that extend EFTs that capture different regimes of the SM. For instance, constructing PETs that extend heavy quark effective theory, which captures the physics of heavy non-relativistic quarks [97–102], and soft-collinear effective theory, which captures the physics of light but highly energetic particles [103–109], would make it possible to apply the factorization approach to hidden particle production in B and D meson decays, where B meson decays are of particular interest due to the persistent B anomalies [110–114].

On the hidden current side, it would be of great use to tabulate hidden current correlation matrices for a number of popular hidden sector models that include particles such as ALPs, HNLs, and dark photons. Since the expressions for the hidden current correlation matrices are observable independent, these tabulated expressions can be used as input for a wide array of master formulae, and could help facilitate *e.g.* global parameter scans that combine constraints from a wide range of observables. Finally, it would be interesting the study the renormalization scale dependence of the reduced matrix elements M_d and the hidden currents J^d , since a robust understanding of this running is necessary in order to combine constraints from observations at multiple characteristic energy scales.

Acknowledgments

The author thanks Dr. Chiara Arina, Prof. Marco Drewes, and Dr. Jan Hajer for interesting discussions and providing valuable feedback regarding the contents of this paper. The work was funded by the Schweizerischer Nationalfonds zur Förderung der wissenschaftlichen Forschung under grant № 200020B-188712.

Appendices

References

- [1] S. Alekhin et al. ‘A facility to Search for Hidden Particles at the CERN SPS: the SHiP physics case’. In: *Rept. Prog. Phys.* 79.12 (2016), p. 124201. DOI: 10.1088/0034-4885/79/12/124201. arXiv: 1504.04855 [hep-ph].
- [2] J. Beacham et al. ‘Physics Beyond Colliders at CERN: Beyond the Standard Model Working Group Report’. In: *J. Phys. G* 47.1 (2020), p. 010501. DOI: 10.1088/1361-6471/ab4cd2. arXiv: 1901.09966 [hep-ex].
- [3] P. Agrawal et al. ‘Feebly-Interacting Particles: FIPs 2020 Workshop Report’ (Feb. 2021). arXiv: 2102.12143 [hep-ph].
- [4] G. Lanfranchi, M. Pospelov, and P. Schuster. ‘The Search for Feebly Interacting Particles’. In: *Ann. Rev. Nucl. Part. Sci.* 71 (2021), pp. 279–313. DOI: 10.1146/annurev-nucl-102419-055056. arXiv: 2011.02157 [hep-ph].
- [5] A. M. Sirunyan et al. ‘A search for pair production of new light bosons decaying into muons in proton-proton collisions at 13 TeV’. In: *Phys. Lett. B* 796 (2019), pp. 131–154. DOI: 10.1016/j.physletb.2019.07.013. arXiv: 1812.00380 [hep-ex].
- [6] A. M. Sirunyan et al. ‘Search for Low-Mass Quark-Antiquark Resonances Produced in Association with a Photon at $\sqrt{s} = 13$ TeV’. In: *Phys. Rev. Lett.* 123.23 (2019), p. 231803. DOI: 10.1103/PhysRevLett.123.231803. arXiv: 1905.10331 [hep-ex].
- [7] S. Mukherjee. ‘Data Scouting and Data Parking with the CMS High level Trigger’. In: *PoS EPS-HEP2019* (2020), p. 139. DOI: 10.22323/1.364.0139.
- [8] G. Aad et al. ‘Measurement of light-by-light scattering and search for axion-like particles with 2.2 nb⁻¹ of Pb+Pb data with the ATLAS detector’. In: *JHEP* 03 (2021), p. 243. DOI: 10.1007/JHEP03(2021)243. arXiv: 2008.05355 [hep-ex].
- [9] R. Aaij et al. ‘Search for Dark Photons Produced in 13 TeV *pp* Collisions’. In: *Phys. Rev. Lett.* 120.6 (2018), p. 061801. DOI: 10.1103/PhysRevLett.120.061801. arXiv: 1710.02867 [hep-ex].
- [10] R. Aaij et al. ‘Search for lepton-flavour-violating decays of Higgs-like bosons’. In: *Eur. Phys. J. C* 78.12 (2018), p. 1008. DOI: 10.1140/epjc/s10052-018-6386-8. arXiv: 1808.07135 [hep-ex].
- [11] R. Aaij et al. ‘Search for $A' \rightarrow \mu^+ \mu^-$ Decays’. In: *Phys. Rev. Lett.* 124.4 (2020), p. 041801. DOI: 10.1103/PhysRevLett.124.041801. arXiv: 1910.06926 [hep-ex].
- [12] R. Aaij et al. ‘Searches for low-mass dimuon resonances’. In: *JHEP* 10 (2020), p. 156. DOI: 10.1007/JHEP10(2020)156. arXiv: 2007.03923 [hep-ex].
- [13] M. Borsato et al. ‘Unleashing the full power of LHCb to probe Stealth New Physics’ (May 2021). arXiv: 2105.12668 [hep-ph].
- [14] R. Aaij et al. ‘Search for heavy neutral leptons in $W^+ \rightarrow \mu^+ \mu^\pm \text{jet}$ decays’. In: *Eur. Phys. J. C* 81.3 (2021), p. 248. DOI: 10.1140/epjc/s10052-021-08973-5. arXiv: 2011.05263 [hep-ex].

- [15] R. Aaij et al. ‘Search for long-lived particles decaying to $e^\pm\mu^\mp\nu$ ’. In: *Eur. Phys. J. C* 81.3 (2021), p. 261. DOI: 10.1140/epjc/s10052-021-08994-0. arXiv: 2012.02696 [hep-ex].
- [16] W. Altmannshofer et al. ‘The Belle II Physics Book’. In: *PTEP* 2019.12 (2019). Ed. by E. Kou and P. Urquijo. [Erratum: *PTEP* 2020, 029201 (2020)], p. 123C01. DOI: 10.1093/ptep/ptz106. arXiv: 1808.10567 [hep-ex].
- [17] J. Liang, Z. Liu, and L. Yang. ‘Belle II constraints on sub-GeV dark matter’ (Nov. 2021). arXiv: 2111.15533 [hep-ph].
- [18] T. Ferber, A. Filimonova, R. Schäfer, and S. Westhoff. ‘Displaced or invisible? ALPs from B decays at Belle II’ (Jan. 2022). arXiv: 2201.06580 [hep-ph].
- [19] X. Cid Vidal et al. ‘Report from Working Group 3: Beyond the Standard Model physics at the HL-LHC and HE-LHC’. In: *CERN Yellow Rep. Monogr.* 7 (2019). Ed. by A. Dainese, M. Mangano, A. B. Meyer, A. Nisati, G. Salam, and M. A. Vesterinen, pp. 585–865. DOI: 10.23731/CYRM-2019-007.585. arXiv: 1812.07831 [hep-ph].
- [20] E. Cortina Gil et al. ‘The Beam and detector of the NA62 experiment at CERN’. In: *JINST* 12.05 (2017), P05025. DOI: 10.1088/1748-0221/12/05/P05025. arXiv: 1703.08501 [physics.ins-det].
- [21] E. Cortina Gil et al. ‘Search for heavy neutral lepton production in K^+ decays’. In: *Phys. Lett. B* 778 (2018), pp. 137–145. DOI: 10.1016/j.physletb.2018.01.031. arXiv: 1712.00297 [hep-ex].
- [22] M. Drewes, J. Hajer, J. Klaric, and G. Lanfranchi. ‘NA62 sensitivity to heavy neutral leptons in the low scale seesaw model’. In: *JHEP* 07 (2018), p. 105. DOI: 10.1007/JHEP07(2018)105. arXiv: 1801.04207 [hep-ph].
- [23] E. Cortina Gil et al. ‘First search for $K^+ \rightarrow \pi^+\nu\bar{\nu}$ using the decay-in-flight technique’. In: *Phys. Lett. B* 791 (2019), pp. 156–166. DOI: 10.1016/j.physletb.2019.01.067. arXiv: 1811.08508 [hep-ex].
- [24] E. Cortina Gil et al. ‘Search for production of an invisible dark photon in π^0 decays’. In: *JHEP* 05 (2019), p. 182. DOI: 10.1007/JHEP05(2019)182. arXiv: 1903.08767 [hep-ex].
- [25] E. Cortina Gil et al. ‘Search for heavy neutral lepton production in K^+ decays to positrons’. In: *Phys. Lett. B* 807 (2020), p. 135599. DOI: 10.1016/j.physletb.2020.135599. arXiv: 2005.09575 [hep-ex].
- [26] E. Cortina Gil et al. ‘Search for a feebly interacting particle X in the decay $K^+ \rightarrow \pi^+X$ ’. In: *JHEP* 03 (2021), p. 058. DOI: 10.1007/JHEP03(2021)058. arXiv: 2011.11329 [hep-ex].
- [27] J. K. Ahn et al. ‘Search for the $K_L \rightarrow \pi^0\nu\bar{\nu}$ and $K_L \rightarrow \pi^0X^0$ decays at the J-PARC KOTO experiment’. In: *Phys. Rev. Lett.* 122.2 (2019), p. 021802. DOI: 10.1103/PhysRevLett.122.021802. arXiv: 1810.09655 [hep-ex].
- [28] J. K. Ahn et al. ‘Search for the $K_L \rightarrow \pi^0\nu\bar{\nu}$ and $K_L \rightarrow \pi^0X^0$ decays at the J-PARC KOTO experiment’. In: *Phys. Rev. Lett.* 122.2 (2019), p. 021802. DOI: 10.1103/PhysRevLett.122.021802. arXiv: 1810.09655 [hep-ex].

- [29] S. Gori, G. Perez, and K. Tobioka. ‘KOTO vs. NA62 Dark Scalar Searches’. In: *JHEP* 08 (2020), p. 110. DOI: 10.1007/JHEP08(2020)110. arXiv: 2005.05170 [hep-ph].
- [30] A. Berlin, S. Gori, P. Schuster, and N. Toro. ‘Dark Sectors at the Fermilab SeaQuest Experiment’. In: *Phys. Rev. D* 98.3 (2018), p. 035011. DOI: 10.1103/PhysRevD.98.035011. arXiv: 1804.00661 [hep-ph].
- [31] C. A. Aidala et al. ‘The SeaQuest Spectrometer at Fermilab’. In: *Nucl. Instrum. Meth. A* 930 (2019), pp. 49–63. DOI: 10.1016/j.nima.2019.03.039. arXiv: 1706.09990 [physics.ins-det].
- [32] J. Alimena et al. ‘Searching for long-lived particles beyond the Standard Model at the Large Hadron Collider’. In: *J. Phys. G* 47.9 (2020), p. 090501. DOI: 10.1088/1361-6471/ab4574. arXiv: 1903.04497 [hep-ex].
- [33] J. P. Chou, D. Curtin, and H. J. Lubatti. ‘New Detectors to Explore the Lifetime Frontier’. In: *Phys. Lett. B* 767 (2017), pp. 29–36. DOI: 10.1016/j.physletb.2017.01.043. arXiv: 1606.06298 [hep-ph].
- [34] D. Curtin et al. ‘Long-Lived Particles at the Energy Frontier: The MATHUSLA Physics Case’. In: *Rept. Prog. Phys.* 82.11 (2019), p. 116201. DOI: 10.1088/1361-6633/ab28d6. arXiv: 1806.07396 [hep-ph].
- [35] J. L. Feng, I. Galon, F. Kling, and S. Trojanowski. ‘ForWard Search Experiment at the LHC’. In: *Phys. Rev. D* 97.3 (2018), p. 035001. DOI: 10.1103/PhysRevD.97.035001. arXiv: 1708.09389 [hep-ph].
- [36] A. Ariga et al. ‘FASER’s physics reach for long-lived particles’. In: *Phys. Rev. D* 99.9 (2019), p. 095011. DOI: 10.1103/PhysRevD.99.095011. arXiv: 1811.12522 [hep-ph].
- [37] V. V. Gligorov, S. Knapen, M. Papucci, and D. J. Robinson. ‘Searching for Long-lived Particles: A Compact Detector for Exotics at LHCb’. In: *Phys. Rev. D* 97.1 (2018), p. 015023. DOI: 10.1103/PhysRevD.97.015023. arXiv: 1708.09395 [hep-ph].
- [38] R. D. Peccei and H. R. Quinn. ‘Constraints Imposed by CP Conservation in the Presence of Instantons’. In: *Phys. Rev. D* 16 (1977), pp. 1791–1797. DOI: 10.1103/PhysRevD.16.1791.
- [39] R. D. Peccei and H. R. Quinn. ‘CP Conservation in the Presence of Instantons’. In: *Phys. Rev. Lett.* 38 (1977), pp. 1440–1443. DOI: 10.1103/PhysRevLett.38.1440.
- [40] S. Weinberg. ‘A New Light Boson?’ In: *Phys. Rev. Lett.* 40 (1978), pp. 223–226. DOI: 10.1103/PhysRevLett.40.223.
- [41] F. Wilczek. ‘Problem of Strong P and T Invariance in the Presence of Instantons’. In: *Phys. Rev. Lett.* 40 (1978), pp. 279–282. DOI: 10.1103/PhysRevLett.40.279.
- [42] J. P. Derendinger, L. E. Ibanez, and H. P. Nilles. ‘On the Low-Energy Limit of Superstring Theories’. In: *Nucl. Phys. B* 267 (1986), pp. 365–414. DOI: 10.1016/0550-3213(86)90396-2.
- [43] G. Lazarides, C. Panagiotakopoulos, and Q. Shafi. ‘Phenomenology and Cosmology With Superstrings’. In: *Phys. Rev. Lett.* 56 (1986), p. 432. DOI: 10.1103/PhysRevLett.56.432.

- [44] S. B. Giddings and A. Strominger. ‘Axion Induced Topology Change in Quantum Gravity and String Theory’. In: *Nucl. Phys. B* 306 (1988), pp. 890–907. DOI: 10.1016/0550-3213(88)90446-4.
- [45] J. Alexander et al. ‘Dark Sectors 2016 Workshop: Community Report’. Aug. 2016. arXiv: 1608.08632 [hep-ph].
- [46] M. Drewes. ‘The Phenomenology of Right Handed Neutrinos’. In: *Int. J. Mod. Phys. E* 22 (2013), p. 1330019. DOI: 10.1142/S0218301313300191. arXiv: 1303.6912 [hep-ph].
- [47] D. Banerjee et al. ‘Search for a Hypothetical 16.7 MeV Gauge Boson and Dark Photons in the NA64 Experiment at CERN’. In: *Phys. Rev. Lett.* 120.23 (2018), p. 231802. DOI: 10.1103/PhysRevLett.120.231802. arXiv: 1803.07748 [hep-ex].
- [48] M. Fabbrichesi, E. Gabrielli, and G. Lanfranchi. ‘The Dark Photon’ (May 2020). DOI: 10.1007/978-3-030-62519-1. arXiv: 2005.01515 [hep-ph].
- [49] W. Buchmüller and D. Wyler. ‘Effective Lagrangian Analysis of New Interactions and Flavor Conservation’. In: *Nucl. Phys. B* 268 (1986), pp. 621–653. DOI: 10.1016/0550-3213(86)90262-2.
- [50] B. Grzadkowski, M. Iskrzynski, M. Misiak, and J. Rosiek. ‘Dimension-Six Terms in the Standard Model Lagrangian’. In: *JHEP* 10 (2010), p. 085. DOI: 10.1007/JHEP10(2010)085. arXiv: 1008.4884 [hep-ph].
- [51] F. Feruglio. ‘The Chiral approach to the electroweak interactions’. In: *Int. J. Mod. Phys. A* 8 (1993), pp. 4937–4972. DOI: 10.1142/S0217751X93001946. arXiv: hep-ph/9301281.
- [52] C. P. Burgess, J. Matias, and M. Pospelov. ‘A Higgs or not a Higgs? What to do if you discover a new scalar particle’. In: *Int. J. Mod. Phys. A* 17 (2002), pp. 1841–1918. DOI: 10.1142/S0217751X02009813. arXiv: hep-ph/9912459.
- [53] B. Grinstein and M. Trott. ‘A Higgs-Higgs bound state due to new physics at a TeV’. In: *Phys. Rev. D* 76 (2007), p. 073002. DOI: 10.1103/PhysRevD.76.073002. arXiv: 0704.1505 [hep-ph].
- [54] R. Barbieri, B. Bellazzini, V. S. Rychkov, and A. Varagnolo. ‘The Higgs boson from an extended symmetry’. In: *Phys. Rev. D* 76 (2007), p. 115008. DOI: 10.1103/PhysRevD.76.115008. arXiv: 0706.0432 [hep-ph].
- [55] D. Barducci et al. ‘Interpreting top-quark LHC measurements in the standard-model effective field theory’ (Feb. 2018). Ed. by J. A. Aguilar-Saavedra, C. Degrande, G. Durieux, F. Maltoni, E. Vryonidou, and C. Zhang. arXiv: 1802.07237 [hep-ph].
- [56] J. Ellis, C. W. Murphy, V. Sanz, and T. You. ‘Updated Global SMEFT Fit to Higgs, Diboson and Electroweak Data’. In: *JHEP* 06 (2018), p. 146. DOI: 10.1007/JHEP06(2018)146. arXiv: 1803.03252 [hep-ph].
- [57] I. Brivio and M. Trott. ‘The Standard Model as an Effective Field Theory’. In: *Phys. Rept.* 793 (2019), pp. 1–98. DOI: 10.1016/j.physrep.2018.11.002. arXiv: 1706.08945 [hep-ph].

- [58] E. Slade. ‘Towards global fits in EFT’s and New Physics implications’. In: *PoS LHCP 2019* (2019). Ed. by P. Roig Garcés, I. Bautista Guzman, A. Fernández Téllez, and M. I. Martínez Hernández, p. 150. DOI: 10.22323/1.350.0150. arXiv: 1906.10631 [hep-ph].
- [59] Z.-Y. Dong, T. Ma, J. Shu, and Y.-H. Zheng. ‘Constructing Generic Effective Field Theory for All Masses and Spins’ (Feb. 2022). arXiv: 2202.08350 [hep-ph].
- [60] I. Brivio, M. B. Gavela, L. Merlo, K. Mimasu, J. M. No, R. del Rey, and V. Sanz. ‘ALPs Effective Field Theory and Collider Signatures’. In: *Eur. Phys. J. C* 77.8 (2017), p. 572. DOI: 10.1140/epjc/s10052-017-5111-3. arXiv: 1701.05379 [hep-ph].
- [61] Y. Liao and X.-D. Ma. ‘Operators up to Dimension Seven in Standard Model Effective Field Theory Extended with Sterile Neutrinos’. In: *Phys. Rev. D* 96.1 (2017), p. 015012. DOI: 10.1103/PhysRevD.96.015012. arXiv: 1612.04527 [hep-ph].
- [62] H.-L. Li, Z. Ren, M.-L. Xiao, J.-H. Yu, and Y.-H. Zheng. ‘Operator bases in effective field theories with sterile neutrinos: $d \leq 9$ ’. In: *JHEP* 11 (2021), p. 003. DOI: 10.1007/JHEP11(2021)003. arXiv: 2105.09329 [hep-ph].
- [63] D. Barducci, E. Bertuzzo, G. G. di Cortona, and G. M. Salla. ‘Dark photon bounds in the dark EFT’. In: *JHEP* 12 (2021), p. 081. DOI: 10.1007/JHEP12(2021)081. arXiv: 2109.04852 [hep-ph].
- [64] M. Duch, B. Grzadkowski, and J. Wudka. ‘Classification of effective operators for interactions between the Standard Model and dark matter’. In: *JHEP* 05 (2015), p. 116. DOI: 10.1007/JHEP05(2015)116. arXiv: 1412.0520 [hep-ph].
- [65] A. De Simone and T. Jacques. ‘Simplified models vs. effective field theory approaches in dark matter searches’. In: *Eur. Phys. J. C* 76.7 (2016), p. 367. DOI: 10.1140/epjc/s10052-016-4208-4. arXiv: 1603.08002 [hep-ph].
- [66] R. Contino, K. Max, and R. K. Mishra. ‘Searching for Elusive Dark Sectors with Terrestrial and Celestial Observations’ (Dec. 2020). arXiv: 2012.08537 [hep-ph].
- [67] J. Aebischer, W. Altmannshofer, E. E. Jenkins, and A. V. Manohar. ‘Dark Matter Effective Field Theory and an Application to Vector Dark Matter’ (Feb. 2022). arXiv: 2202.06968 [hep-ph].
- [68] V. Cirigliano, M. L. Graesser, and G. Ovanessian. ‘WIMP-nucleus scattering in chiral effective theory’. In: *JHEP* 10 (2012), p. 025. DOI: 10.1007/JHEP10(2012)025. arXiv: 1205.2695 [hep-ph].
- [69] A. L. Fitzpatrick, W. Haxton, E. Katz, N. Lubbers, and Y. Xu. ‘The Effective Field Theory of Dark Matter Direct Detection’. In: *JCAP* 02 (2013), p. 004. DOI: 10.1088/1475-7516/2013/02/004. arXiv: 1203.3542 [hep-ph].
- [70] M. Cirelli, E. Del Nobile, and P. Panci. ‘Tools for model-independent bounds in direct dark matter searches’. In: *JCAP* 10 (2013), p. 019. DOI: 10.1088/1475-7516/2013/10/019. arXiv: 1307.5955 [hep-ph].
- [71] M. Hoferichter, P. Klos, and A. Schwenk. ‘Chiral power counting of one- and two-body currents in direct detection of dark matter’. In: *Phys. Lett. B* 746 (2015), pp. 410–416. DOI: 10.1016/j.physletb.2015.05.041. arXiv: 1503.04811 [hep-ph].

- [72] M. Hoferichter, P. Klos, J. Menéndez, and A. Schwenk. ‘Analysis strategies for general spin-independent WIMP-nucleus scattering’. In: *Phys. Rev. D* 94.6 (2016), p. 063505. DOI: 10.1103/PhysRevD.94.063505. arXiv: 1605.08043 [hep-ph].
- [73] F. Bishara, J. Brod, B. Grinstein, and J. Zupan. ‘Chiral Effective Theory of Dark Matter Direct Detection’. In: *JCAP* 02 (2017), p. 009. DOI: 10.1088/1475-7516/2017/02/009. arXiv: 1611.00368 [hep-ph].
- [74] F. Bishara, J. Brod, B. Grinstein, and J. Zupan. ‘From quarks to nucleons in dark matter direct detection’. In: *JHEP* 11 (2017), p. 059. DOI: 10.1007/JHEP11(2017)059. arXiv: 1707.06998 [hep-ph].
- [75] M. Hoferichter, P. Klos, J. Menéndez, and A. Schwenk. ‘Nuclear structure factors for general spin-independent WIMP-nucleus scattering’. In: *Phys. Rev. D* 99.5 (2019), p. 055031. DOI: 10.1103/PhysRevD.99.055031. arXiv: 1812.05617 [hep-ph].
- [76] J. C. Criado, A. Djouadi, M. Pérez-Victoria, and J. Santiago. ‘A complete Effective Field Theory for Dark Matter’ (Apr. 2021). arXiv: 2104.14443 [hep-ph].
- [77] C. Arina, J. Hajer, and P. Klose. ‘Portal Effective Theories. A framework for the model independent description of light hidden sector interactions’. In: *JHEP* 09 (2021), p. 063. DOI: 10.1007/JHEP09(2021)063. arXiv: 2105.06477 [hep-ph].
- [78] J. Alwall, P. Schuster, and N. Toro. ‘Simplified Models for a First Characterization of New Physics at the LHC’. In: *Phys. Rev. D* 79 (2009), p. 075020. DOI: 10.1103/PhysRevD.79.075020. arXiv: 0810.3921 [hep-ph].
- [79] D. Alves. ‘Simplified Models for LHC New Physics Searches’. In: *J. Phys. G* 39 (2012). Ed. by N. Arkani-Hamed et al., p. 105005. DOI: 10.1088/0954-3899/39/10/105005. arXiv: 1105.2838 [hep-ph].
- [80] J. Abdallah et al. ‘Simplified Models for Dark Matter Searches at the LHC’. In: *Phys. Dark Univ.* 9-10 (2015), pp. 8–23. DOI: 10.1016/j.dark.2015.08.001. arXiv: 1506.03116 [hep-ph].
- [81] H. K. Dreiner, H. E. Haber, and S. P. Martin. ‘Two-component spinor techniques and Feynman rules for quantum field theory and supersymmetry’. In: *Phys. Rept.* 494 (2010), pp. 1–196. DOI: 10.1016/j.physrep.2010.05.002. arXiv: 0812.1594 [hep-ph].
- [82] P. A. Zyla et al. ‘Review of Particle Physics’. In: *PTEP* 2020.8 (2020), p. 083C01. DOI: 10.1093/ptep/ptaa104.
- [83] J. Gasser and H. Leutwyler. ‘Chiral Perturbation Theory: Expansions in the Mass of the Strange Quark’. In: *Nucl. Phys. B* 250 (1985), pp. 465–516. DOI: 10.1016/0550-3213(85)90492-4.
- [84] S. P. Martin. ‘TASI 2011 lectures notes: two-component fermion notation and supersymmetry’. *Theoretical Advanced Study Institute in Elementary Particle Physics: The Dark Secrets of the Terascale*. 2013, pp. 199–258. DOI: 10.1142/9789814390163_0005. arXiv: 1205.4076 [hep-ph].
- [85] V. Cirigliano, G. Ecker, H. Neufeld, A. Pich, and J. Portoles. ‘Kaon Decays in the Standard Model’. In: *Rev. Mod. Phys.* 84 (2012), p. 399. DOI: 10.1103/RevModPhys.84.399. arXiv: 1107.6001 [hep-ph].

- [86] E. Fermi. ‘Trends to a Theory of beta Radiation’. Italian. In: *Meeting of the Italian School of Physics and Weak Interactions Bologna, Italy, April 26-28, 1984*. Vol. 11. 535. 1934, pp. 1–19. DOI: 10.1007/BF02959820.
- [87] E. E. Jenkins, A. V. Manohar, and M. Trott. ‘Renormalization Group Evolution of the Standard Model Dimension Six Operators I: Formalism and lambda Dependence’. In: *JHEP* 10 (2013), p. 087. DOI: 10.1007/JHEP10(2013)087. arXiv: 1308.2627 [hep-ph].
- [88] E. E. Jenkins, A. V. Manohar, and M. Trott. ‘Renormalization Group Evolution of the Standard Model Dimension Six Operators II: Yukawa Dependence’. In: *JHEP* 01 (2014), p. 035. DOI: 10.1007/JHEP01(2014)035. arXiv: 1310.4838 [hep-ph].
- [89] R. Alonso, E. E. Jenkins, A. V. Manohar, and M. Trott. ‘Renormalization Group Evolution of the Standard Model Dimension Six Operators III: Gauge Coupling Dependence and Phenomenology’. In: *JHEP* 04 (2014), p. 159. DOI: 10.1007/JHEP04(2014)159. arXiv: 1312.2014 [hep-ph].
- [90] J. S. Schwinger. ‘Chiral dynamics’. In: *Phys. Lett. B* 24 (1967), pp. 473–476. DOI: 10.1016/0370-2693(67)90277-8.
- [91] J. A. Cronin. ‘Phenomenological model of strong and weak interactions in chiral $U(3) \times U(3)$ ’. In: *Phys. Rev.* 161 (1967), pp. 1483–1494. DOI: 10.1103/PhysRev.161.1483.
- [92] J. Wess and B. Zumino. ‘Lagrangian method for chiral symmetries’. In: *Phys. Rev.* 163 (1967), pp. 1727–1735. DOI: 10.1103/PhysRev.163.1727.
- [93] S. Weinberg. ‘Dynamical approach to current algebra’. In: *Phys. Rev. Lett.* 18 (1967), pp. 188–191. DOI: 10.1103/PhysRevLett.18.188.
- [94] S. Weinberg. ‘Nonlinear realizations of chiral symmetry’. In: *Phys. Rev.* 166 (1968), pp. 1568–1577. DOI: 10.1103/PhysRev.166.1568.
- [95] R. F. Dashen and M. Weinstein. ‘Soft pions, chiral symmetry, and phenomenological lagrangians’. In: *Phys. Rev.* 183 (1969), pp. 1261–1291. DOI: 10.1103/PhysRev.183.1261.
- [96] S. Gasiorowicz and D. A. Geffen. ‘Effective Lagrangians and field algebras with chiral symmetry’. In: *Rev. Mod. Phys.* 41 (1969), pp. 531–573. DOI: 10.1103/RevModPhys.41.531.
- [97] M. A. Shifman and M. B. Voloshin. ‘On Production of d and D^* Mesons in B Meson Decays’. In: *Sov. J. Nucl. Phys.* 47 (1988). [*Yad. Fiz.* 47, 801], p. 511.
- [98] N. Isgur and M. B. Wise. ‘Weak Decays of Heavy Mesons in the Static Quark Approximation’. In: *Phys. Lett. B* 232 (1989), pp. 113–117. DOI: 10.1016/0370-2693(89)90566-2.
- [99] H. Georgi. ‘An Effective Field Theory for Heavy Quarks at Low-energies’. In: *Phys. Lett. B* 240 (1990), pp. 447–450. DOI: 10.1016/0370-2693(90)91128-X.
- [100] N. Isgur and M. B. Wise. ‘Weak Transition Form-Factors between Heavy Mesons’. In: *DPF Conf.1990:0459-464*. Vol. B237. 1990, pp. 527–530. DOI: 10.1016/0370-2693(90)91219-2.
- [101] B. Grinstein. ‘The Static Quark Effective Theory’. In: *Nucl. Phys. B* 339 (1990), pp. 253–268. DOI: 10.1016/0550-3213(90)90349-I.

- [102] A. F. Falk, H. Georgi, B. Grinstein, and M. B. Wise. ‘Heavy Meson Form-factors From QCD’. In: *Nucl. Phys. B* 343 (1990), pp. 1–13. DOI: 10.1016/0550-3213(90)90591-Z.
- [103] C. W. Bauer, S. Fleming, and M. E. Luke. ‘Summing Sudakov logarithms in $B \rightarrow X(s\gamma)$ in effective field theory’. In: *Phys. Rev. D* 63 (2000), p. 014006. DOI: 10.1103/PhysRevD.63.014006. arXiv: hep-ph/0005275 [hep-ph].
- [104] C. W. Bauer, S. Fleming, D. Pirjol, and I. W. Stewart. ‘An Effective field theory for collinear and soft gluons: Heavy to light decays’. In: *Phys. Rev. D* 63 (2001), p. 114020. DOI: 10.1103/PhysRevD.63.114020. arXiv: hep-ph/0011336 [hep-ph].
- [105] C. W. Bauer and I. W. Stewart. ‘Invariant operators in collinear effective theory’. In: *Phys. Lett. B* 516 (2001), pp. 134–142. DOI: 10.1016/S0370-2693(01)00902-9. arXiv: hep-ph/0107001 [hep-ph].
- [106] C. W. Bauer and A. V. Manohar. ‘Shape function effects in $B \rightarrow X(s)\gamma$ and $B \rightarrow X(u)l\bar{\nu}$ decays’. In: *Phys. Rev. D* 70 (2004), p. 034024. DOI: 10.1103/PhysRevD.70.034024. arXiv: hep-ph/0312109 [hep-ph].
- [107] S. W. Bosch, B. O. Lange, M. Neubert, and G. Paz. ‘Factorization and shape function effects in inclusive B meson decays’. In: *Nucl. Phys. B* 699 (2004), pp. 335–386. DOI: 10.1016/j.nuclphysb.2004.07.041. arXiv: hep-ph/0402094 [hep-ph].
- [108] M. Beneke, F. Campanario, T. Mannel, and B. D. Pecjak. ‘Power corrections to $\bar{B} \rightarrow X(u)l\bar{\nu}(X(s)\gamma)$ decay spectra in the ‘shape-function’ region’. In: *JHEP* 06 (2005), p. 071. DOI: 10.1088/1126-6708/2005/06/071. arXiv: hep-ph/0411395 [hep-ph].
- [109] C. W. Bauer, A. Hornig, and F. J. Tackmann. ‘Factorization for generic jet production’. In: *Phys. Rev. D* 79 (2009), p. 114013. DOI: 10.1103/PhysRevD.79.114013. arXiv: 0808.2191 [hep-ph].
- [110] S. Descotes-Genon, J. Matias, and J. Virto. ‘Understanding the $B \rightarrow K^*\mu^+\mu^-$ Anomaly’. In: *Phys. Rev. D* 88 (2013), p. 074002. DOI: 10.1103/PhysRevD.88.074002. arXiv: 1307.5683 [hep-ph].
- [111] W. Altmannshofer and D. M. Straub. ‘New Physics in $B \rightarrow K^*\mu\mu$?’. In: *Eur. Phys. J. C* 73 (2013), p. 2646. DOI: 10.1140/epjc/s10052-013-2646-9. arXiv: 1308.1501 [hep-ph].
- [112] R. Aaij et al. ‘Test of lepton universality with $B^0 \rightarrow K^{*0}\ell^+\ell^-$ decays’. In: *JHEP* 08 (2017), p. 055. DOI: 10.1007/JHEP08(2017)055. arXiv: 1705.05802 [hep-ex].
- [113] R. Aaij et al. ‘Test of lepton universality in beauty-quark decays’ (Mar. 2021). arXiv: 2103.11769 [hep-ex].
- [114] J. Alda, J. Guasch, and S. Penaranda. ‘Anomalies in B mesons decays: Present status and future collider prospects’. *International Workshop on Future Linear Colliders*. May 2021. arXiv: 2105.05095 [hep-ph].